This manuscript was accepted by Phys. Plasmas. Click here to see the version of record.

Suppression of Diamagnetism by Neutrals Pressure in Partially Ionized, High-Beta Plasma

Shunjiro Shinohara,[1,a)] Daisuke Kuwahara,[1)] , Kazuki Yano,[2)] and Amnon Fruchtman[3)]

[1]*Division of Advanced Mechanical Systems Engineering, Institute of Engineering, Tokyo University of Agriculture and Technology, 2-24-16, Naka-cho, Koganei, Tokyo 184-8588, Japan*

[2]*Department of Mechanical Systems Engineering, The Graduate School of Engineering, Tokyo University of Agriculture and Technology, 2-24-16, Naka-cho, Koganei, Tokyo 184-8588, Japan*

[3]*Department of Physics, Faculty of Sciences, H. I. T. - Holon Institute of Technology, 52 Golomb Street, Holon 58102, Israel*

Suppression of diamagnetism in partially ionized plasma with high beta was experimentally investigated by the use of Langmuir and Hall sensor probes, focusing on a neutrals pressure effect. The plasma beta, which is the ratio of plasma to vacuum magnetic pressures, varied from ~ 1 % to > 100 % while the magnetic field varied from ~ 120 G to 1 G. Here, a uniform magnetized argon plasma was operated mostly in an inductive mode, using a helicon plasma source of the Large Helicon Plasma Device (LHPD) [S. Shinohara *et al*., Phys. Plasmas **16**, 057104 (2009)] with a diameter of 738 mm and an axial length of 4,860 mm. Electron density varied from 5×10^{15} m^{-3} to $< 3\times10^{18}$ m^{-3}, while an argon fill pressure was varied from ~ 0.02 Pa to 0.75 Pa as well as the magnetic field mentioned above, with the fixed radio frequency (rf) and power of 7 MHz and ~ 3.5 kW, respectively. The observed magnetic field reduction ratio, a decrease of the magnetic field divided by the vacuum one, was up to 18 %. However, in a certain parameter regime, where the product of ion and electron Hall terms is a key parameter, the measured diamagnetic effect was smaller than expected by the plasma beta. This suppressed diamagnetism is explained by the neutrals pressure replacing magnetic pressure in balancing plasma pressure. Diamagnetism is weakened if neutrals pressure is comparable to the plasma pressure and if the coupling of plasma and neutrals pressures by ion-neutral collisions is strong enough.

I. INTRODUCTION

Diamagnetism is a fundamental characteristic of plasmas. When the plasma is of high β, defined here as $2\mu_0 p/B_0^2$ (p being the plasma pressure, and here, the maximal plasma pressure, B_0 vacuum magnetic field, μ_0 vacuum permeability), diamagnetism governs the interaction of the plasma with magnetic fields by modifying the fields inherently. Examples include magnetic fusion and propulsion devices, e.g., the MagnetoPlasmaDynamics (MPD) thruster. A high β plasma exhibits nonlinear interesting behaviors in various equilibria and instabilities such as mirror and firehose instabilities.[1] Wave phenomena also can change when β is more than a mass ratio of electron to ion.[2] Thus the high β affects

a) Electronic mail: sshinoha@cc.tuat.ac.jp

ACCEPTED MANUSCRIPT

AIP Publishing

This manuscript was accepted by Phys. Plasmas. Click here to see the version of record.

the cross field transport, sometimes showing a complex combination of electromagnetic and electrostatic characteristics with large amplitudes. In nuclear fusion mirror machines, Alfvén Ion Cyclotron Instabilities (AIC) were observed[3] for a relatively low β of a few %. In space, magnetic field dip or peak types in the magnetic mirror structures can be found in a shock sheath layer as well as a magnetic hole in a solar wind.[4]

Although high β value could be achieved in magnetic fusion tokamaks such as spherical tokamaks, it is still limited by less than several tens of % except for Field Reversal Configuration (FRC) of having ~ 100 %. On the other hand, the electron density n_e in helicon plasma sources[5] can be high (typically $n_e \sim 10^{19}$ m^{-3}) even for a low magnetic field with a few kW radio frequency (rf) power, so that high β plasma can be easily reached. Therefore, helicon plasma sources allow experiments with high beta plasma and can contribute to the understanding of the important phenomena that are hard to explore experimentally otherwise. Note that when helicon plasma sources are used with a weak magnetic field, their mode of operation often is that of inductively coupled, weakly magnetized, rf discharges.

Here, we will discuss the diamagnetic effect, which is one of characteristics of a high beta plasma, from a balance between various pressures. In the ideal Magnetohydrodynamic (MHD) conditions with a fully ionized plasma, a complete expulsion of the magnetic field from the plasma interior can be expected when $\beta = 1$. Here, in this discussion, the MHD conditions may be considered as follows: (i) both the ion and electron Larmor radii, ρ_i and ρ_e, respectively, are much less than the plasma radius a and (ii) the Hall parameter of $H = \omega_c \tau >> 1$ for both ions and electrons (ω_c: angular cyclotron frequency, τ: collision time). Here, concerning the collisions, we must take note of ion-neutral collisions for ions and electron-neutral and electron-ion collisions for electrons. This complete expulsion comes from pressure balance: $B_0^2/2\mu_0 = B^2/2\mu_0 + p_e + p_i$ (total pressure is constant across the plasma region).[1] Here, p_e (p_i) is an electron (ion) pressure in the presence of plasmas, and total plasma pressure $p = p_e + p_i$. In other words, the magnetic field reduction rate $R = |\Delta B/B_0|$ is expressed as $R_I = 1-\sqrt{1-\beta}$ from the above pressure balance, where $\Delta B < 0$ is a decrease of the magnetic field relative to B_0.

Contrary to this expected diamagnetism, a few publications[6-8] on high beta helicon plasma sources reported magnetic reduction rate R that was much smaller than R_I. Scime *et al.*[6] have shown very weak diamagnetic effect with observed low frequency, electromagnetic waves, which are consistent with the AIC instabilities. Here, R was < 10 % in a range of $B_0 \sim$ a few tens of G even though high electron beta β_e of 1,000 % was achieved. Note that an electron temperature T_e is much higher than an ion temperature T_i in helicon/rf discharges, and thus $\beta_e >>$ ion beta of β_i where $\beta = \beta_e + \beta_i$. Corr and Boswell[7] also observed a very small value of $R \sim 2$ % ($B_0 \sim 34$ G) in spite of high β_e of ~ 200 %. Shinohara *et al.*[8] have also shown a small value of $R \sim 4.5$ % ($B_0 \sim 50$ G) with high β_e of < 80 % even though $R_I \sim 50$ % is expected. Concerning the dc plasma

ACCEPTED MANUSCRIPT

AIP Publishing

This manuscript was accepted by Phys. Plasmas. Click here to see the version of record.

production method[9] instead of using helicon sources, a magnetic hole was formed in the plasma interior with $\beta_e \sim 500$ % under the very weak field $B_0 \sim 5$ G, where ions are not magnetized with the relatively high electron density ($n_e < 10^{18}$ m^{-3}). However, R was only ~ 15 % with $\beta_e = 100$ %, which again deviates from the above prediction of the diamagnetic effect R_I (R should have been 1 in this case). Although the above reports suggested explanations for the measured low diamagnetism, magnetic field penetration[7] or an excitation of a radial electric field,[9] the suppressed diamagnetism is still an important and not sufficiently understood phenomenon.

Here, it is suggested that neutrals pressure could play a dominant role in diamagnetism suppression. Neutrals depletion that is often predicted for high-density helicon plasmas[10-12] results in a finite gradient of neutrals pressure. In contrast to MHD conditions with fully ionized plasmas mentioned above, in such partially ionized plasmas, neutrals pressure cannot be neglected in the total pressure balance. A total pressure balance w/ and w/o plasmas is then expressed in a universal form, i.e., $B_0^2 / 2\mu_0 + p_{n0} = B^2 / 2\mu_0 + p_e + p_i + p_n$. Here, p_{no} and p_n are neutrals pressures w/o and w/ plasmas, respectively. This leads to the magnetic reduction rate $R_{II} = 1 - \sqrt{1 - \beta - \Delta\beta_n}$, where $\Delta\beta_n = (p_n - p_{n0}) / (B_0^2 / 2\mu_0) = \beta_n - \beta_{n0}$ (β_n and β_{n0} are neutrals beta w/ and w/o the plasma, respectively), which is generally a negative value in the plasma core. From this formula, a neutrals pressure decrease in plasmas, neutrals depletion, weakens the diamagnetic effect. Note that the MHD equilibrium shows $\nabla p = \mathbf{j} \times \mathbf{B}$,[1] and this p of $p_e + p_i$ can be replaced for $p_e + p_i + p_n$ in the presence of the neutrals pressure. Therefore, the effect of a relatively large neutrals depletion on the plasma diamagnetism must be considered.

In the present work, noting the possible role of neutrals pressure, we have investigated the diamagnetic effect in high-beta rf plasmas by the use of a helicon plasma source, mostly operated in an inductive mode, varying systematically an argon fill pressure and the axial magnetic field. Simple model analysis of the diamagnetic field has been also executed to elucidate a neutrals pressure effect experimentally observed. The outline of the present paper is as follows: First, in Sec. II, formulation of the model analysis on neutrals effect is presented. In Sec. III, the experimental setup of the Large Diameter Helicon Device (LHPD)[13] is described briefly. In Sec. IV, experimental results of high beta plasma characteristics with a comparison to results by model analysis on neutrals effect is presented, focusing on plasma diamagnetic effect. Finally, conclusions with discussions are given in Sec. V.

II. FORMULARTION OF ANALYSIS

We assume azimuthally-symmetric partially-ionized cylindrical plasma that is immersed in a magnetic field parallel to the axis of symmetry denoted z axis. The length of the cylindrical plasma is much larger than its radius, so that radial ambipolar cross-field transport is dominant. As motion along magnetic field lines is neglected, the problem becomes one-

ACCEPTED MANUSCRIPT

AIP Publishing

This manuscript was accepted by Phys. Plasmas. Click here to see the version of record.

dimensional where all variables depend on the distance from the axis r only. The plasma is described by fluid equations where T_i is assumed much smaller than T_e.

The steady-state governing equation for the quasi-neutral plasma is the continuity equation,

$$\frac{1}{r}\frac{\partial(r\Gamma)}{\partial r} = \beta_{ion} N n_e, \tag{1}$$

and the momentum equation, neglecting both electron and ion inertia,

$$T_e \frac{\partial n_e}{\partial r} = -\left(\frac{eB\omega_c}{\nu_e} + m_i \nu_i\right)\Gamma. \tag{2}$$

Here, Γ is the ambipolar plasma particle flux density towards the radial wall and $N = p_n/T_g$ is the neutrals density (T_g being the neutral-gas temperature). The ionization rate coefficient is $\beta_{ion} = \sigma_0 v_{te} \exp(-\epsilon_i/T_e)$,[14] where $v_{te} \equiv (8T_e/\pi m_e)^{1/2}$ is the electron thermal velocity (m_e being the electron mass) and $\sigma_0 \equiv \pi(e^2/4\pi\epsilon_0\epsilon_i)^2$, ϵ_0 being the vacuum permittivity and ϵ_i the ionization energy. For argon, the parameters are $\sigma_0 = 2.67 \times 10^{-20}\text{m}^2$ and $\epsilon_i = 15.6$ eV. The electron cyclotron angular frequency is $\omega_c = eB/m_e$, the ion-neutrals collision frequency is $\nu_i = k_{iN}N$, while the electron collision frequency, $\nu_e = k_{eN}N + k_{ei}n_e$, is the sum of the electron collision frequencies with neutrals and with ions. The electron-neutral collision rate constant for argon is $k_{eN} = 1.28 \times 10^{-13}\ \text{m}^3\text{s}^{-1}$.[14] The electron-ion Coulomb collision rate constant is taken as $k_{ei} = 2.9 \times 10^{-12}\ln\Lambda\, T_e^{-3/2}(\text{eV})^{3/2}\ \text{m}^3\text{s}^{-1}$,[15] where $\ln\Lambda = 10$ is used. Neutrals depletion is caused by the drag on neutrals by ion collisions. Since the cross section for ion-neutral collision depends on their relative velocity and has some uncertainty, we present here numerical calculations with two sets of values of k_{iN}. In one calculation, the ion-neutral collision rate constant for argon was taken as $k_{iN} = 6.3 \times 10^{-16}\ \text{m}^3\text{s}^{-1}$,[14] while in another calculation we used a value that is 3.5 larger for comparison.

The momentum equation for the neutrals is

$$T_g \frac{\partial N}{\partial r} - m_i \nu_i \Gamma = 0. \tag{3}$$

Neutral-gas pressure gradient is balanced by the drag by the ions. It is assumed here that the total number of neutrals per unit length, $N_T = \pi a^2 p_{n0}/T_g$, is not changed by that drag. Here a is the radius of the discharge chamber. Since p_{n0} is the gas pressure without discharge, $N_0 \equiv p_{n0}/T_g$ is the neutrals density without the discharge. It is also assumed that the ionization is not high enough as to reduce N_T during the discharge, although the plasma pressure $p_e = n_e T_e$ can be comparable to the gas pressure (it is assumed that T_e is much higher than the T_i so that $p_e >> p_i$).

The electron azimuthal diamagnetic current results, by Ampere's law, in a gradient of the magnetic field, $\partial B/\partial r = (\mu_0 e\omega_c/\nu_e)\Gamma$ (μ_0 is the vacuum permeability and e elementary charge). Combining this expression for the magnetic field

ACCEPTED MANUSCRIPT

AIP Publishing

This manuscript was accepted by Phys. Plasmas. Click here to see the version of record.

gradient with Eqs. (2) and (3), we obtain the total pressure balance (the ion pressure is neglected),

$$n_e T_e + \frac{B^2}{2\mu_0} + NT_g = \frac{B_0^2}{2\mu_0} + N_0 T_g. \tag{4}$$

It is assumed that at the wall $n_e = 0$, $N = N_0$, and $B = B_0$. Both T_e and T_g are assumed uniform.

From Eq. (4), the diamagnetism is expressed as $R = R_{II}$, where, because T_g is assumed uniform and constant, $R_{II} = 1 - \sqrt{1 - \beta + \beta_{n0} D}$. Here, $D \equiv 1 - N(0)/N_0$ is defined as the neutrals depletion, which was discussed in the introduction. It is clear that the diamagnetism is determined by $\beta - \beta_{n0} D$, and a significant neutrals pressure relative to the plasma pressure combined with significant neutrals depletion suppresses the diamagnetism.

Equations (1) - (4) are the governing equations for Γ, n_e, N, and B as functions of $r \in [0, a]$. The boundary conditions are $\Gamma(0) = 0, n_e(0) = n_0$ and $n_e(a) = 0$, $\int_0^a 2\pi r N dr = N_T$, and $B(a) = B_0$, where n_0, N_T, and B_0 (and T_g) are specified. Since n_e is specified both on axis and at the wall, T_e is an eigenvalue of the problem.

When β is small enough, so that the neutrals depletion D and the diamagnetic effect R_{II} are small, we write $R_{II} \cong (\beta - \beta_{n0} D)/2$. We can solve the equations in this case analytically in a perturbative way. To zeroth order, the neutrals density and the magnetic field are assumed constant, so that Eqs. (1) and (2) are combined in a standard way to $(1/r)(\partial/\partial r)(r \partial n_e/\partial r) = -[\alpha(C+1)/a^2] n_e$, where $\alpha \equiv \beta m_i \nu_i N_0 a^2 / T_e$ and

$$C \equiv \frac{e^2 B_0^2}{m_i m_e \nu_i \nu_e}. \tag{5}$$

The coefficients α and C are taken as constant (in calculating ν_e the electron density is taken as n_0). Using the boundary condition $n_e(a) = 0$, we write the plasma density and particle flux density as $n_e = n_0 J_0(p_1 r/a)$ and $\Gamma = (n_0 T_e / [m_i \nu_i a(C+1)]) p_1 J_1(p_1 r/a)$. Here, J_0 and J_1 are the Bessel functions of the zeroth and the first order, respectively, and $p_1 = 2.4048$ is the first zero of J_0. The resulting solvability condition, $\sqrt{\alpha(C+1)} = p_1$, determines the value of the eigenvalue T_e. The perturbed neutrals density and magnetic field are obtained using the zeroth order expressions for n_e and for Γ. To the first order, the neutrals density is $N = N_0 - \left[(n_0 T_e/T_g)/(C+1)\right] J_0(p_1 r/a)$, while the magnetic field is $B = B_0 - [(\mu_0 n_0 T_e/B_0) C/(C+1)] J_0(p_1 r/a)$. Defining $\Delta N = N_0 - N(0)$ and $\Delta B = B_0 - B(0)$, we find that

$$D = \frac{1}{(C+1)} \frac{\beta}{\beta_{n0}}, \quad R_{II} = \frac{C}{(C+1)} \frac{\beta}{2}. \tag{6}$$

It is seen that when $C \gg 1$, the diamagnetic effect is noticeable, $R_{II} = \Delta B/B_0 \cong \beta/2 \gg \beta_{n0} D$, while $D = \Delta N/N_0 \ll \beta/\beta_{n0}$. Conversely, when $C \ll 1$, the diamagnetic effect is small, $R_{II} = \Delta B/B_0 \ll \beta/2$, while the neutrals pressure-gradient due to neutrals depletion is large and balances the plasma pressure, $D = \Delta N/N_0 \cong \beta/\beta_{n0}$.

ACCEPTED MANUSCRIPT

AIP Publishing

This manuscript was accepted by Phys. Plasmas. Click here to see the version of record.

For the calculation in this paper, we specify B_0, N_T, n_0, and the radius a. The total number of neutrals N_T is specified through p_{n0} and T_g, and we assume that N_T and T_g are not changed by the discharge. The peak plasma density n_0 is deduced from the probe measurements. We then use the above equations to find $B(r), N(r), n(r)$, and a uniform T_e although the measured T_e has a small variation with r. The amounts of diamagnetism and of neutrals depletion are obtained from $B(r)$ and $N(r)$. As concluded from the linear analysis, the parameter C indicates whether diamagnetism is expected to be suppressed by neutrals depletion.

We should note that due to various approximate assumptions, such as retaining radial transport only, the model is expected to recover the experimental results approximately only.

III. EXPERIMENTAL SETUP

In the LHPD experiment, a large-diameter (738 mm) chamber with an axial length of 4,860 mm was used, at the Institute of Space and Astronautical Science (ISAS), Japan Aerospace Exploration Agency (JAXA), where the plasma production efficiency is very high.[16] In typical experiments, ion and electron Hall parameters, H_i and H_e, are much smaller than 1, and much larger than 1, respectively, and $B \sim 10$ G corresponds to ion Larmor radius $\rho_i \sim a$ while electron Larmor radius ρ_e is much smaller than a (electrons are magnetized). Note that with low magnetic field the source operates in inductive mode instead of helicon mode.

Figure 1 shows a schematic view of LHPD, in which a high-density plasma is produced by a spiral antenna,[13] with 4 turns and a 430 mm in outer diameter, located on the RHS of this device in this figure. The typical rf power and its frequency are $P_{rf} \sim 3.5$ kW and $f = 7$ MHz, respectively, with a pulsed duration of 40 ms with a repetition rate of one pulse per second (pps). An argon fill pressure was controlled by a mass flow controller and a needle valve, located in the central region of the device, in a low (< 0.13 Pa) and high (> 0.13 Pa) pressure regions, respectively, and a neutral pressure before discharges are measured by an ionization gauge on the RHS of the device. Here, n_e and T_e are measured by a Langmuir probe and the magnetic field by Hall sensor probes (A1324, Allegro Micro Systems), which are inserted from side ports at z (axial direction from the end flange, facing a spiral antenna through a quartz window) = 1,480 mm, as shown in this figure. Figure 2 shows a detailed structure of Hall sensor probes with a sensitivity of 5 mV/G (effective Least Square Bit (LSB) in the present experiment is 0.02 G) and a frequency response of 17 kHz. Two channels of the Hall sensor inside a SUS316 pipe with opposite polarities can measure the axial component of the magnetic field, which can check the common mode noise.

Data were averaged over the later half of an rf discharge, i.e., for 20 ms, with four shots. The axial magnetic field less than 120 G was applied in this experiment, and the measuring position is in a nearly uniform magnetic-field region.[16]

ACCEPTED MANUSCRIPT

AIP Publishing

This manuscript was accepted by Phys. Plasmas. Click here to see the version of record.

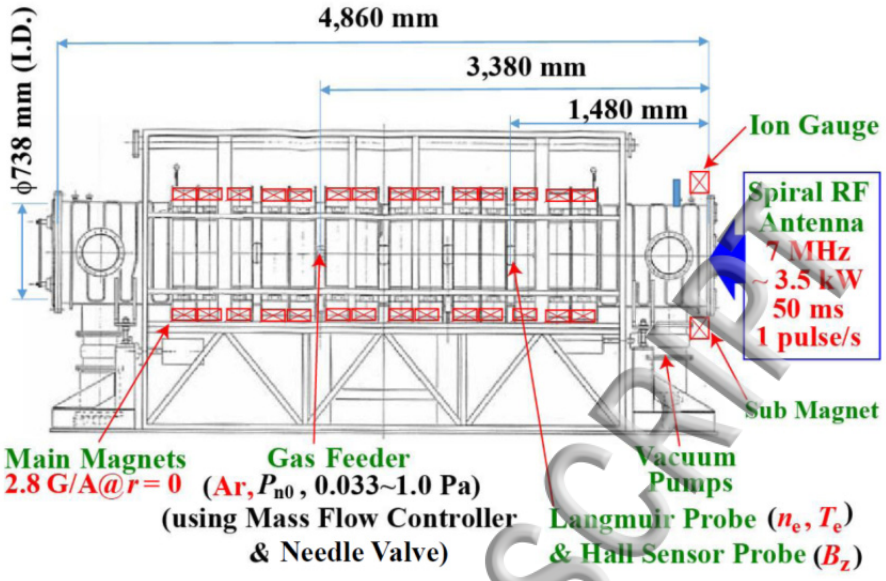

FIG. 1. Schematic view of LHPD.

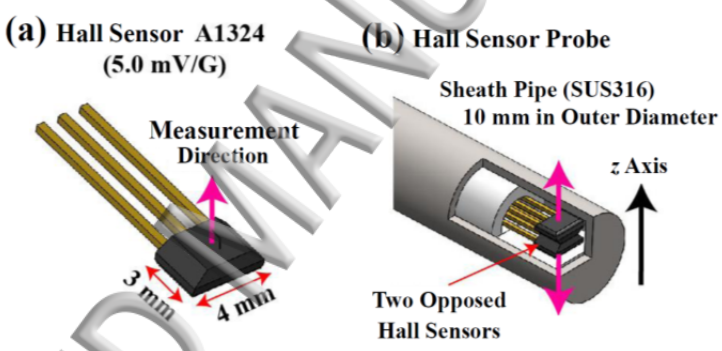

FIG. 2. Structures of (a) Hall sensor element and (b) completed Hall sensor probes.

IV. EXPERIMENTAL RESULTS

First, we will present typical data of T_e and n_e by taking current-voltage characteristics before showing high-beta plasma characteristics, showing diamagnetism. Figure 3 shows T_e and n_e as a function of radius, at different fill pressure P_0 (before a discharge) with P_{rf}~ 3.5 kW and B_0 = 7.6 G. Note that the inner radius of the chamber is 369 mm. There was a tendency that T_e decreased with radius gradually and also with P_0, from the maximum value of ~ 5.3 eV near the center with P_0 = 0.02 Pa to the minimum one to ~ 1.2 eV near the edge with P_0 = 0.75 Pa, in the pressure range of 0.02-0.75 Pa. Concerning n_e, which is shown in a logarithmic scale in (b), it also decreased with radius and it was higher with the lower P_0 except for 0.02 Pa.

In some cases, we took data of ion saturation current I_{is} only. In these cases, we have derived n_e, interpolating T_e data which we have taken. Note that this procedure is considered to make a small deviation from a real central value of n_e as well

ACCEPTED MANUSCRIPT

AIP Publishing

This manuscript was accepted by Phys. Plasmas. Click here to see the version of record.

as p_e and also β. If T_e is larger than a real value by 15 (30) %, n_e is expected to be smaller than a real one by 7.2 (14) %, since I_{is} is measured experimentally and it is proportional to the product of n_e and square root of T_e. Plasma pressure, which is almost the same as the electron pressure p_e, is thus only 7.2 (14) % increase. Since β is proportional to p_e, it also increases by 7.2 (14) %.

Hereafter, unless otherwise specified,

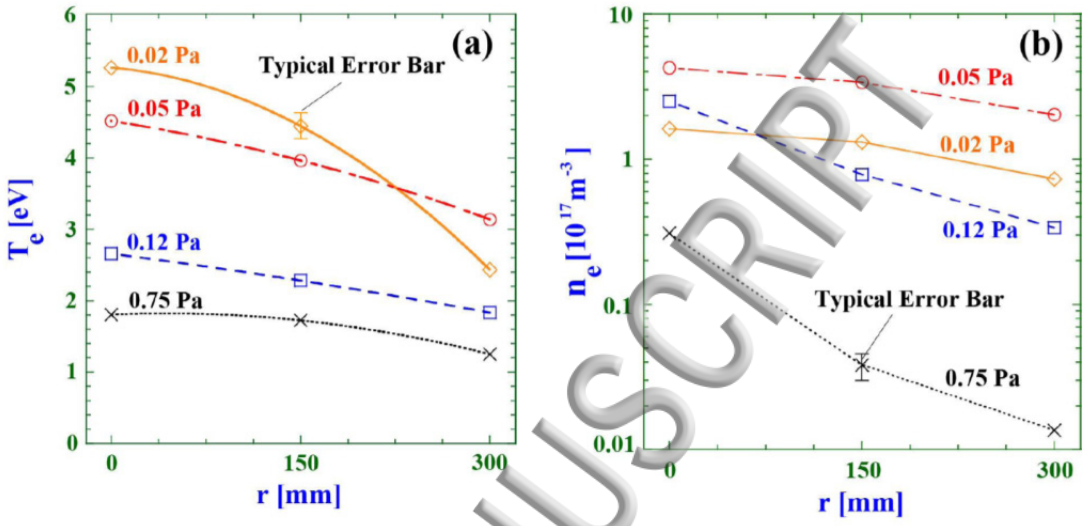

measurements of T_e and n_e have been carried out at a radial position of r = 20 mm, which is near the plasma center.

FIG. 3. Radial profiles of (a) T_e and (b) n_e at different P_0. Here, curves are written for an eye guide.

Next we will show n_e and β as a function of B_0 at different P_0. As shown in Fig. 4 (a), with an increase in B_0 and decrease in P_0, n_e increased, and it was in a range of ~ (0.5-2.5)$\times 10^{15}$ m^{-3} and ~ (2-3)$\times 10^{18}$ m^{-3} in the cases of $B_0 < 1$ G and 120 G, respectively. Figure 4 (b) shows that β (in the central plasma region where the maximum value is expected) ~ β_e (since T_i is much smaller than T_e) mostly decreased with increasing B_0. This is because n_e increased slower than B_0^2 as B_0 increased, as shown in Fig. 4 (a), and β was larger than unity in the very weak B region of < 1-2 G. Here, β was higher in a

ACCEPTED MANUSCRIPT

This manuscript was accepted by Phys. Plasmas. Click here to see the version of record.

low pressure range because of higher n_e, as is also shown in Fig. 4 (a). There is a dip of β near B_0 = 10 G, which may corresponds to $\rho_i \sim a$.

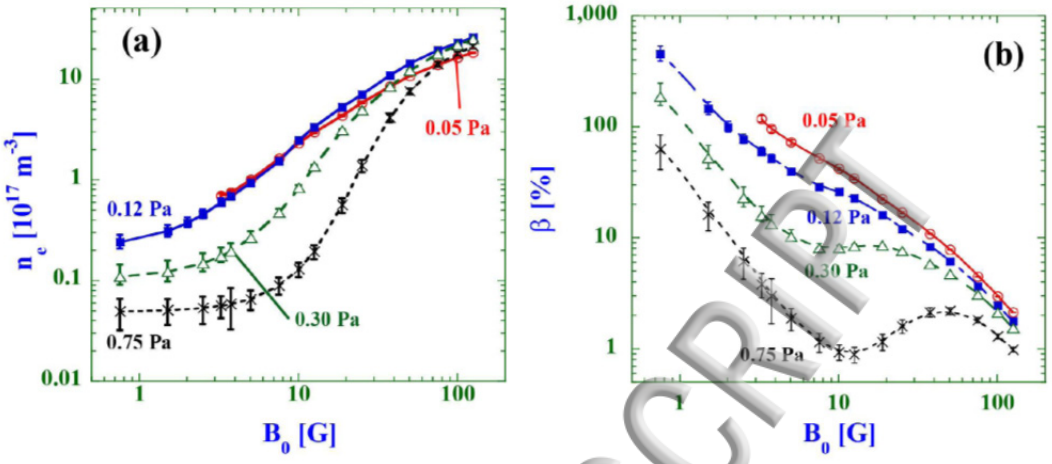

FIG. 4. (a) n_e and (b) β as a function of B_0 at different P_0.

Figure 5 (a) shows $R = |\Delta B/B_0|$ as a function of P_0 at different B_0. Large error bars in low B_0 cases come partly from the very small change (absolute value) of the magnetic field. It can be clearly seen that R increased with lowering P_0 and/or B_0, and it was up to 18 % in the low P_0 and B_0 values. Combining data of Fig. 4 (b) and 5 (a), a dependence of R on P_0 was derived, as shown in Fig. 5 (b), along with a theoretical curve $R_I = 1-\sqrt{1-\beta}$, neglecting a neutrals pressure effect discussed above. For the low P_0 and/or low β (it means the higher B_0 region), there is a good agreement between experimental data and the curve of R_I. However, there is a deviation from this curve in the higher β region (low magnetic field region), and a deviation region of β increased with the higher P_0, which will be discussed later from a viewpoint of the neutrals pressure effect.

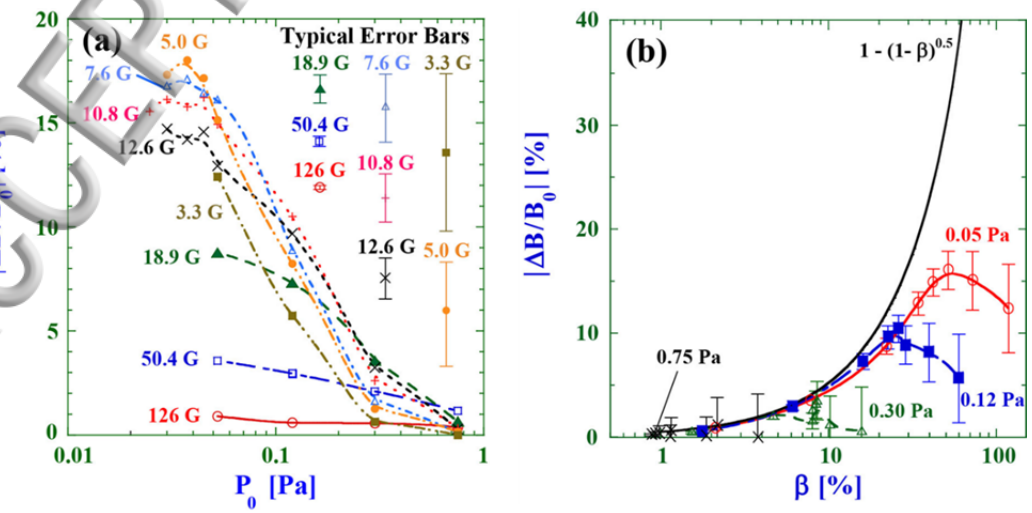

ACCEPTED MANUSCRIPT

AIP Publishing

This manuscript was accepted by Phys. Plasmas. Click here to see the version of record.

FIG. 5. Field reduction ratio of R experimentally obtained (a) as a function of P_0, changing B_0 and (b) as a function of β, changing P_0. Here, a theoretical curve of R_I, neglecting a neutrals pressure, is also shown in (b).

It has to be noted that the high beta region in Fig. 5 (b) is the region of low plasma density, as can be seen in Fig. 4. Reducing the magnetic field results in a decrease of the n_e; however, n_e decreases slower than B_0^2, therefore β increases, as was mentioned. The region of high beta in Fig. 5 (b) is therefore a region where the plasma pressure p is low and is comparable or even smaller than the neutrals pressure p_n. This shows that p_n plays a role in the suppression of diamagnetism if it is comparable to the plasma pressure, and this is further supported by the occurrence of the suppression for specified magnetic field at a lower beta (and a higher plasma pressure) when the gas pressure is higher. The neutrals effect is further demonstrated in Fig. 6.

For comparison, here, a model for neutrals depletion in plasma in a uniform magnetic field[16] was extended to allow a nonuniform field due to the diamagnetic effect, as was described in the former section of II, and the more detailed discussion will be published elsewhere. The model was used to estimate R and a neutral depletion in the plasma core in order to make a comparison to the experimental results. We have used equations of total pressure balance mentioned above and Ampere's law in addition to continuity, momentum, and magnetic flux conservation. By linearizing these equations, the following governing parameter C is derived: $C = e^2 B_0^2 / (m_e m_i \nu_i \nu_e)$ from Eq. (5), which is also written as $H_e H_i$, using Hall parameters. The diamagnetic effect expressed as R_I is dominant when $C >> 1$ (it means fewer collisions and higher field), while in the opposite limit the use of R_{II} instead of R_I is necessary. This comes from the relation of $R_{II} = (\beta/2)\, C / (1 + C)$ from Eq. (6).

Figure 6 shows a dependence of R on B_0, changing P_0, along with two calculation results by the use of $R_{II} = 1-\sqrt{1-\beta-\Delta\beta_n}$, shown above, choosing a standard ion-neutral collision frequency ν_i from ref. 14 and an enhanced frequency by a factor of 3.5, as was mentioned, while other collision data ν_e are also from ref. 14. Moreover, a theoretical curve of $R_I = 1-\sqrt{1-\beta}$ is shown for comparison. Note that large error bars in low B_0 cases in (b)-(d) partly come from the very small change of the magnetic field, as was mentioned. Despite certain simplifying assumptions in the model, there is a good agreement, especially in a lower P_0 condition, between experiments and calculated R_{II}, using two values of ν_i in almost all B_0 values down to weak B_0 of ~ 3 G. In the lower and higher P_0 regions, this agreement is better based on the enhanced and standard ion-neutral collisions ν_i, respectively. Note that a theoretical R_I, neglecting a neutrals pressure effect, can describe the experimentally obtained diamagnetic effect only in the higher B_0 region of more than a few tens of G. Although the

ACCEPTED MANUSCRIPT

This manuscript was accepted by Phys. Plasmas. Click here to see the version of record.

neutrals pressure was not obtained experimentally, the calculated results describe well the characteristics of the diamagnetism. The model is nonlinear; nevertheless the value of C, a parameter that results from a linear analysis, provides a good indication as to how strong the neutrals pressure effect is. As is seen in the figure, C increases with the increase of B_0, and decreases with the decrease of P_0; C = 1 when B_0 = 5.5 (35) G for P_0 = (0.12) 0.75 Pa, denotes well where the deviation occurs between curves of experimental values of R and curves of R_I.

In Fig. 6, for a large B_0, the diamagnetic effect is caused as expected by the plasma pressure. As the magnetic field is reduced, R increases following the increase of β. However, R reaches a maximum and for lower B, R decreases despite the increase of β, reflecting suppression of the diamagnetic effect. The value of B_0 where R is maximal roughly separates the regions of diamagnetism and suppressed diamagnetism. Using Fig. 4, we find that the maximal R occurs at p of ~ (0.10-0.12) Pa for P_0 = 0.05, 0.12, 0.3, and 0.75 Pa. As expected, p_n suppresses diamagnetism once it is approaching p. This p_n being comparable to p is a necessary but not sufficient condition. The coupling between the plasma and the neutrals gas has to be strong enough, so that depletion of neutrals is large enough to suppress the diamagnetism.

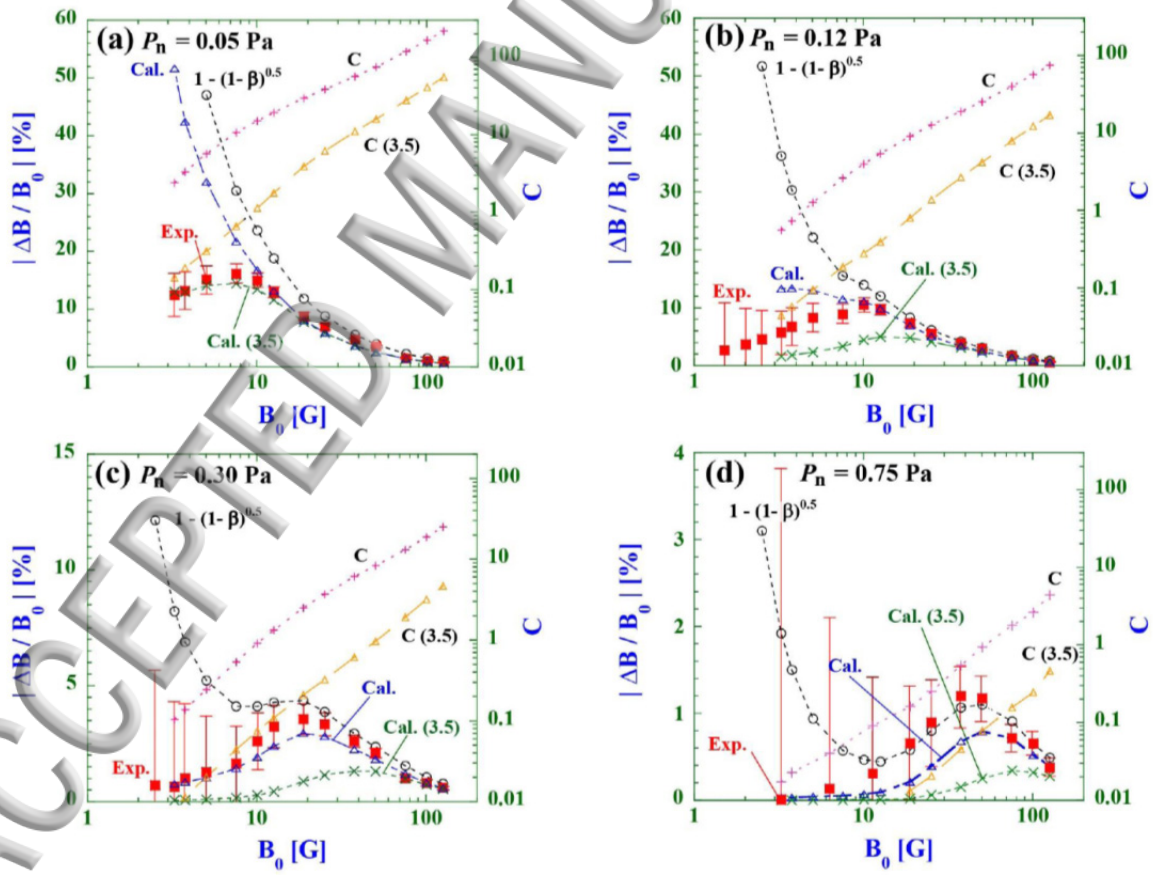

FIG. 6. Dependence of R from experiments on B_0 in the case of P_0 = (a) 0.05, (b) 0.12, (c) 0.30, and (d) 0.75 Pa. R_{II} = $1-\sqrt{1-\beta-\Delta\beta_n}$ found by a theoretical model that includes neutrals pressure is shown for two different values of the ion-

ACCEPTED MANUSCRIPT

AIP Publishing

This manuscript was accepted by Phys. Plasmas. Click here to see the version of record.

neutral collision frequency, the second larger by 3.5 than the first frequency. $R_I = 1-\sqrt{1-\beta}$ for measured β is shown as well. For comparison, curves of C are also shown.

Next, we will examine the spatial profiles of the diamagnetic effect. Figure 7 shows two examples of radial profiles of ΔB with P_0 = 0.05 Pa, showing that R in the plasma center were ~ 12 % and ~ 14 % in the cases of B_0 = 3.3 G and 5.0 G, respectively. Here, n_e in the center were ~ 0.98×10^{17} m^{-3} and ~ 0.63×10^{17} m^{-3}, respectively, and β in the center were ~ 100 % and 67 %, respectively, for B_0 = 3.3 G and 5.0 G. Note that while ΔB is negative in an inner plasma region, it is positive outside the plasma (inner vacuum wall radius is 369 mm) due to a conservation of the total magnetic flux inside the region of the magnetic coils. For comparison, a standard and an enhanced ν_i values are used in deriving calculated curves for both cases. Again, we can see a good agreement between experiments and a model, which includes p_n by the use of an enhanced ν_i values. Note that it is found that a neutrals density is depleted in the center by this calculation (not shown in this figure).

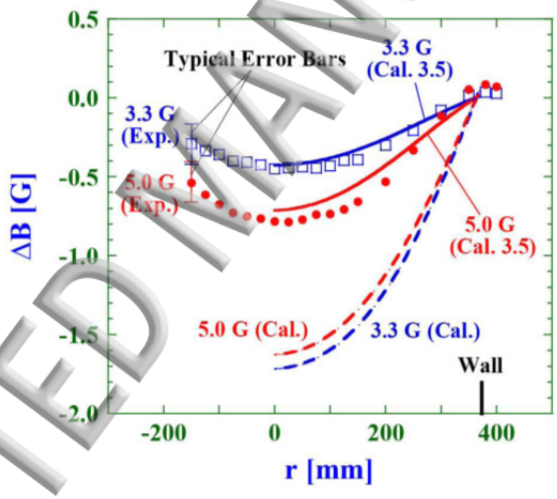

FIG. 7. Radial profiles of the diamagnetic effect ΔB in the cases of B_0 = 3.3 (open blue squares) and 5.0 (closed red circles) G with P_0 = 0.05 Pa from the experiments. Here, a calculation conditions including a neutral effect were the same as in Fig. 6.

V. DISCUSSIONS AND CONCLUSIONS

In this paper, we have investigated the diamagnetic effect (R < 20 %) in low ~ high beta (up to β > 100 %) plasmas, using a high-density (up to ~ 10^{18} m^{-3}) rf source in the weak field region (from ~ 1 to 120 G). The weakening of the diamagnetism from the MHD expectation of R_I can be interpreted by the use of a simple equilibrium model (R_{II}) from a total pressure balance including a neutrals pressure in addition to magnetic and plasma pressures, regardless of the β value and an

ACCEPTED MANUSCRIPT

AIP Publishing

This manuscript was accepted by Phys. Plasmas. Click here to see the version of record.

ionization ratio. Namely, a low diamagnetic effect can be understood in terms of a neutrals pressure change (control parameter is C), during a discharge.

Note that this diamagnetic effect was also investigated by the Large Mirror Device (LMD)[18] (inner diameter of 445 mm with 1,700 mm axial length). Under the conditions of B_0 = 25 and 50 G with P_0 = 0.2 Pa, we have injected P_{rf} of ~ 2 kW with an f of 7 MHz. The experimentally obtained R was ~ 6.0 % and ~ 3.2 % in the case of B_0 = 25 G and 50 G, respectively. Here, n_e near the central region were ~ 1.1×10^{18} m^{-3} and ~ 2.5×10^{18} m^{-3}, respectively, and β near the central region were ~ 20 % and ~ 12 %, respectively, in the cases of B_0 = 25 G and 50 G. While the expected R_I was ~ 7.8 % and ~ 4.6 %, respectively, for the above two sets of the magnetic field, R_{II} was ~ 6.7 % and ~ 3.8 %, respectively, from the simple calculation using the standard ν_I value. Here, we have assumed the typical T_e of 3-5 eV in this experiment. Although R_I values are relatively close to the experimental values, again R_{II} curves are more close to the experimental data, showing a neutrals pressure effect is important.

In order to have a further analysis, concerning a neutrals (depletion) density profile, which is a key to understand the diamagnetic effect in high-density, high-beta plasma studies, it is necessary to measure this pressure directly using, e.g., a manometer[10] and Two Photon Absorption Laser Induced Fluorescence (TALIF)[19], or developing a Collisional Radiative (CR) model[20] to estimate this indirectly. Needless to say, detailed, spatial profiles of basic data of n_e, T_e, and B in addition to the plasma potential are also important.

ACKNOWLEDGMENTS

Our LHPD experiments were conducted in and supported by at ISAS, JAXA as a collaborative program with the Space Chamber Laboratory. A. F. was supported by the Japan Society for the Promotion of Science (JSPS) Invitation Fellowship under Contract No. S14033, and by the Israel Science Foundation, Grant no. 765/11.

REFERENCES

[1]K. Miyamoto, *Plasma Physics for Nuclear Fusion* (The MIT Press, Cambridge, 1979).

[2]D. Leneman, W. Gekelman, and J. Maggs, Phys. Rev. Lett. **82**, 2673 (1999).

[3]M. Ichimura, M. Inutake, T. Katanuma, N. Hino, H. Hojo, K. Ishii, T. Tamano, and S. Miyoshi, Phys. Rev. Lett. **70**, 2734 (1993).

[4]B. T. Tsurutani, G. S. Lakhina, O. P. Verkhoglyadova, E. Echer, F. L. Guamieri, Y. Narita, and D. O. Constantinescu, J. Geophys. Res. **116**, A02103 (2011).

[5]R.W. Boswell, Phys. Lett. **33**A, 457 (1970).

ACCEPTED MANUSCRIPT

AIP Publishing

This manuscript was accepted by Phys. Plasmas. Click here to see the version of record.

[6]E. E. Scime, P. A. Keiter, M. M. Balkey, R. F. Boivin, J. L. Kline, and M. Blackburn, Phys. Plasmas **7**, 2157 (2000).

[7]C. S. Corr and R. W. Boswell, Phys. Plasmas **14**, 122503 (2007).

[8]S. Shinohara, T. Motomura, K. Tanaka, T. Tanikawa, and K. P. Shamrai, Plasma Sources Sci. Technol. **19**, 034018 (2010).

[9]R. Stenzel and J. M. Urrutia, Phys. Plasmas **7**, 4450 (2000).

[10]J. Gilland, R. Breun, and N. Hershkowitz, Plasma Sources Sci. Technol. **7**, 416 (1998).

[11]S. Cho, Phys. Plasmas **6**, 359 (1999).

[12]A. Fruchtman, G. Makrinich, P. Chabert, and J. M. Rax, Phys. Rev. Lett. **95**, 115002 (2005).

[13]S. Shinohara and T. Tanikawa, Rev. Sci. Instrum. **75**, 1941 (2004).

[14]M. A. Lieberman and A. J. Lichtenberg, *Principles of Plasma Discharges and Materials Processing* (Wiley, New York, 1994).

[15] J. D. Huba, *NRL Plasma Formulary*, Revised 2016, P. 28.
http://www.nrl.navy.mil/ppd/content/nrl-plasma-formulary

[16]S. Shinohara, T. Hada, T. Motomura, K. Tanaka, T. Tanikawa, K. Toki, Y. Tanaka, and K. P. Shamrai, Phys. Plasmas **16**, 057104 (2009).

[17]A. Fruchtman, Plasma Sources Sci. Technol. **18**, 025033 (2009).

[18]S. Shinohara, S. Takechi, and Y. Kawai, Jpn. J. Appl. Phys. **35**, 4503 (1996).

[19]R. M. Magee, M. E. Galante, N. Gulbrandsen, D. W. McCarren, and E. E. Scime, Phys. Plasmas **21**, 123506 (2012).

[20]J. Vlček, J. Phys. D: Appl. Phys. **22**, 623 (1989).

ACCEPTED MANUSCRIPT

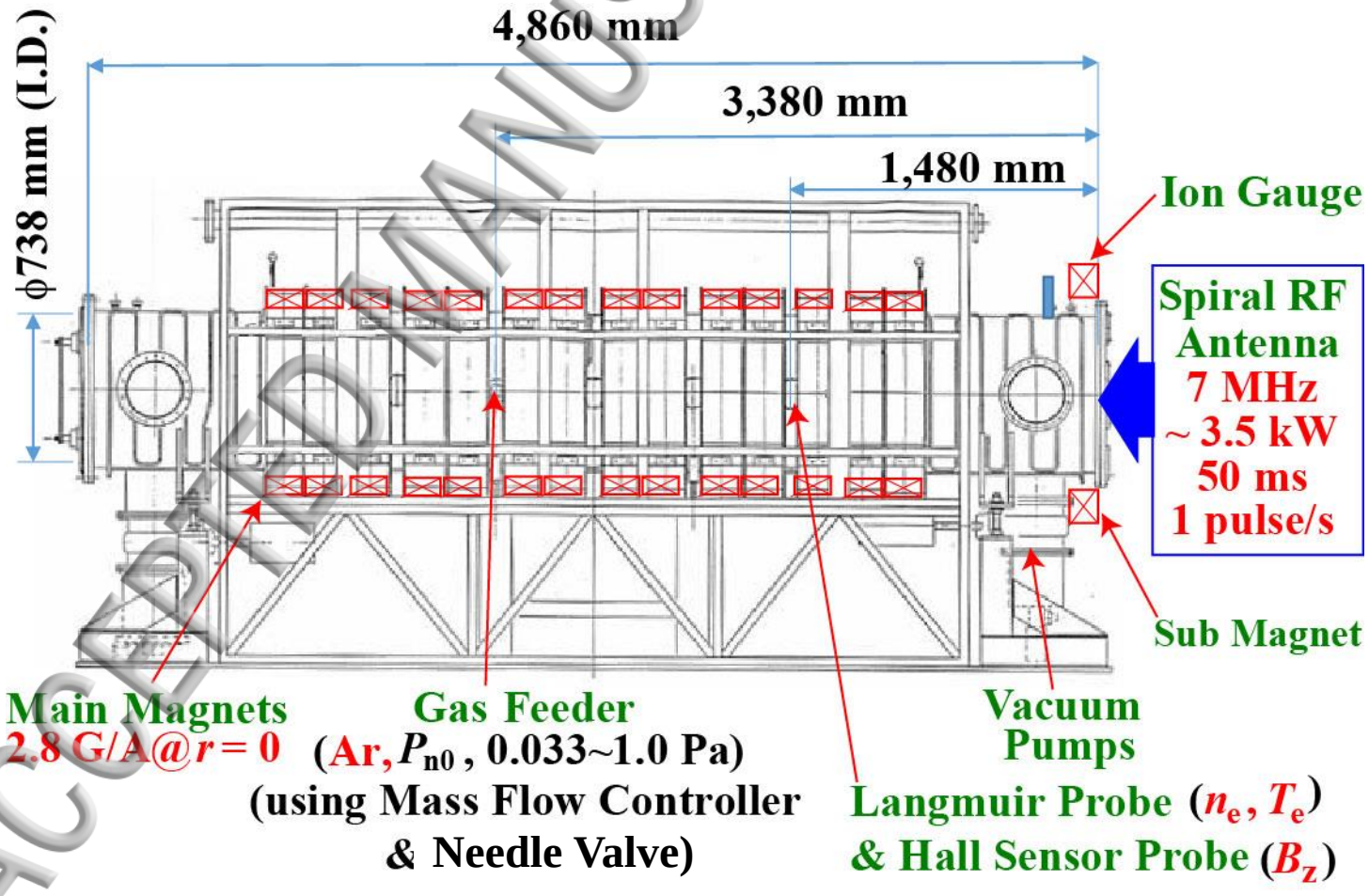

Fig. 1

ACCEPTED MANUSCRIPT

ACCEPTED MANUSCRIPT

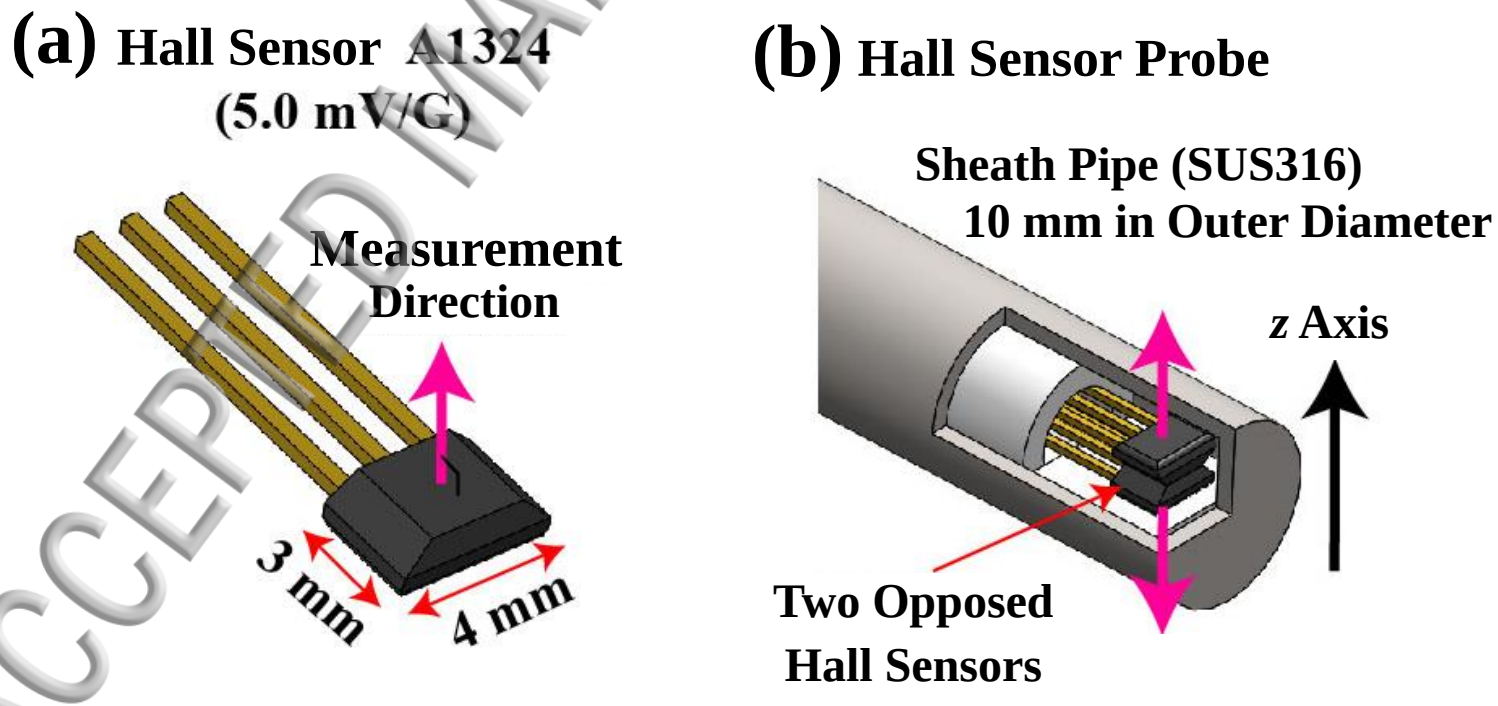

Fig. 2

ACCEPTED MANUSCRIPT

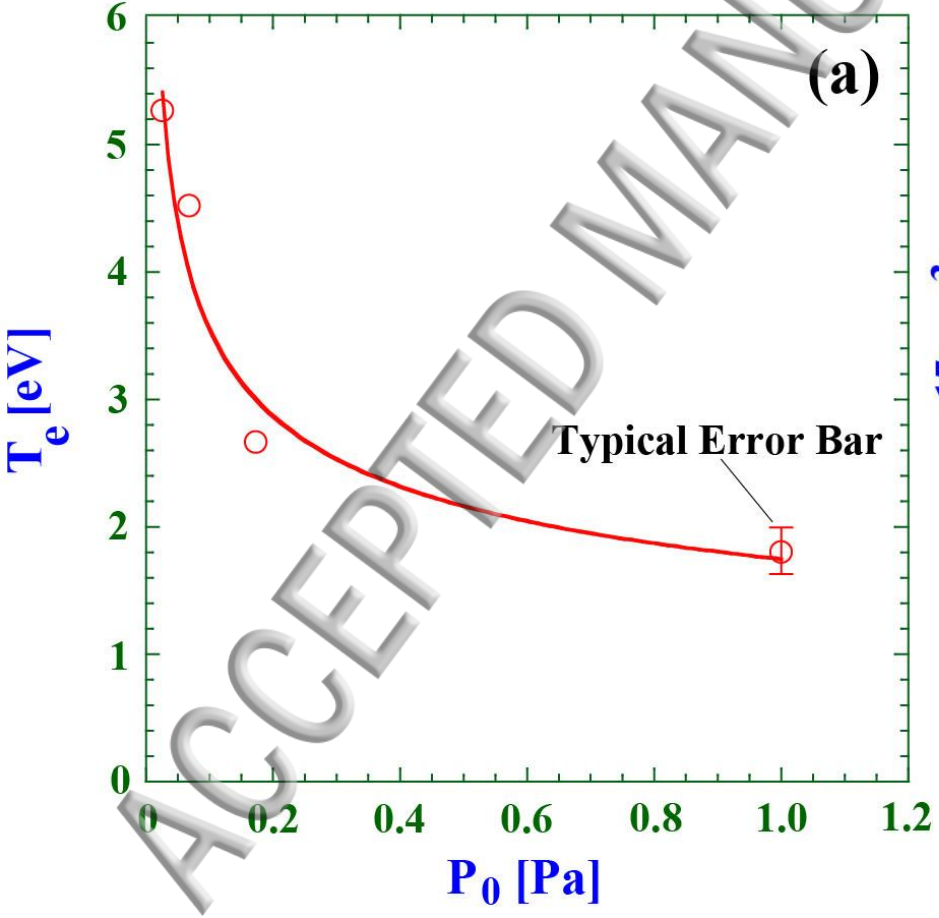

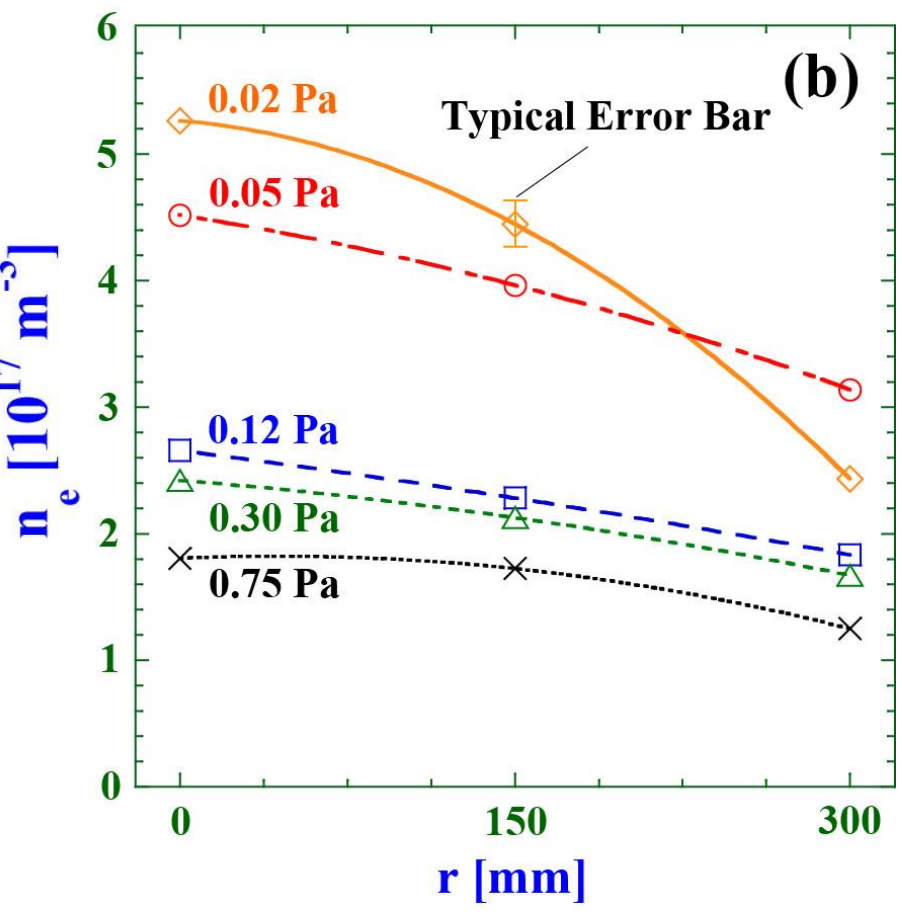

Fig. 3

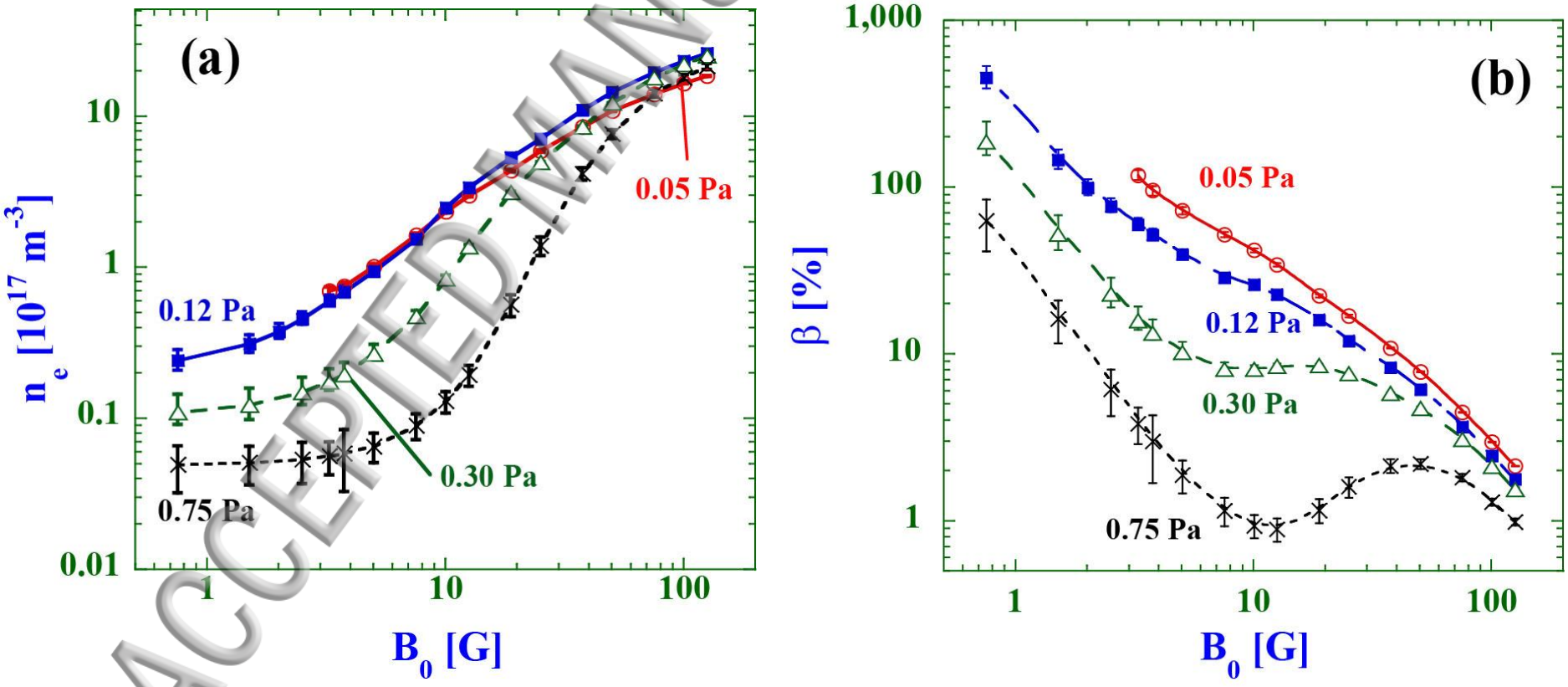

ACCEPTED MANUSCRIPT

Fig. 4

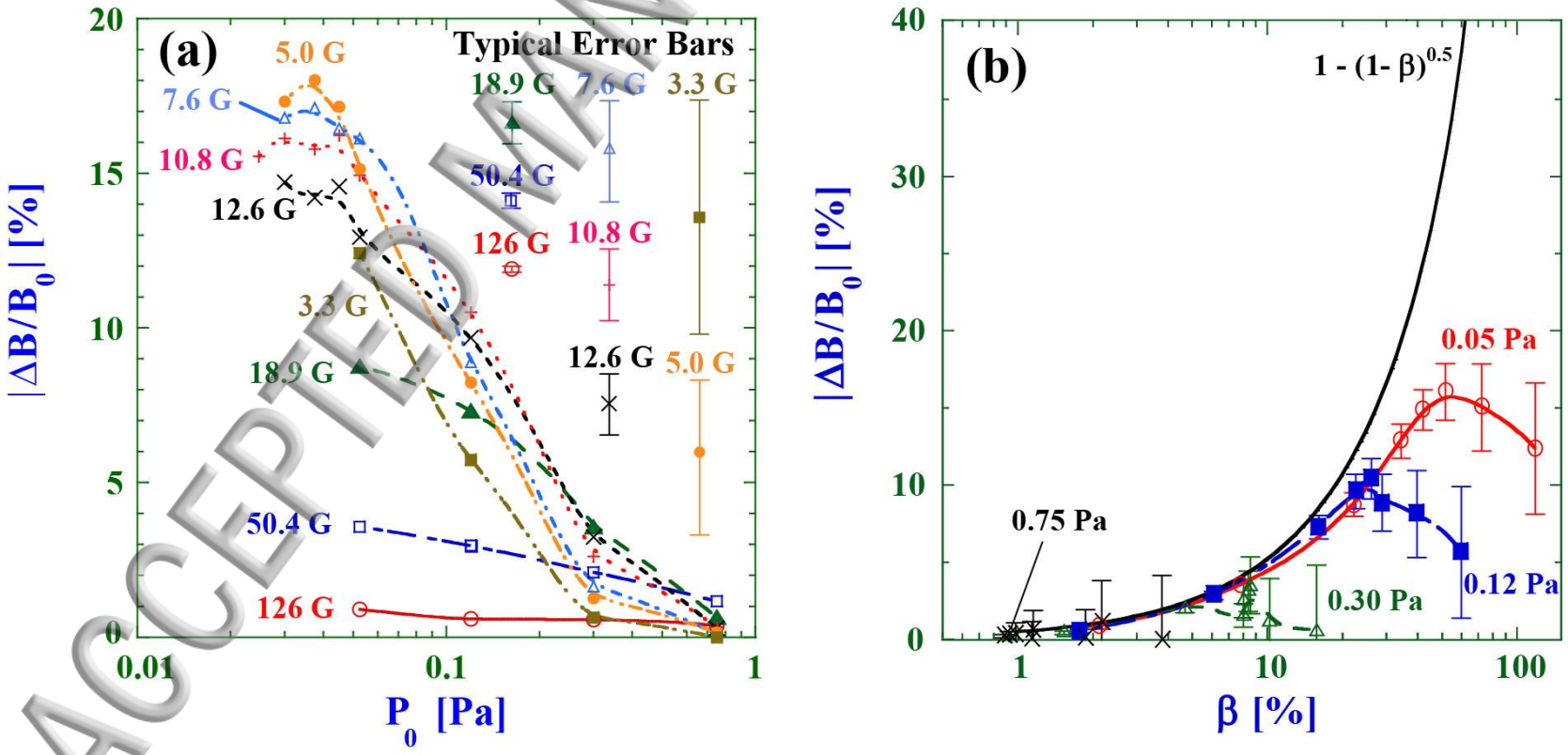

Fig. 5

ACCEPTED MANUSCRIPT

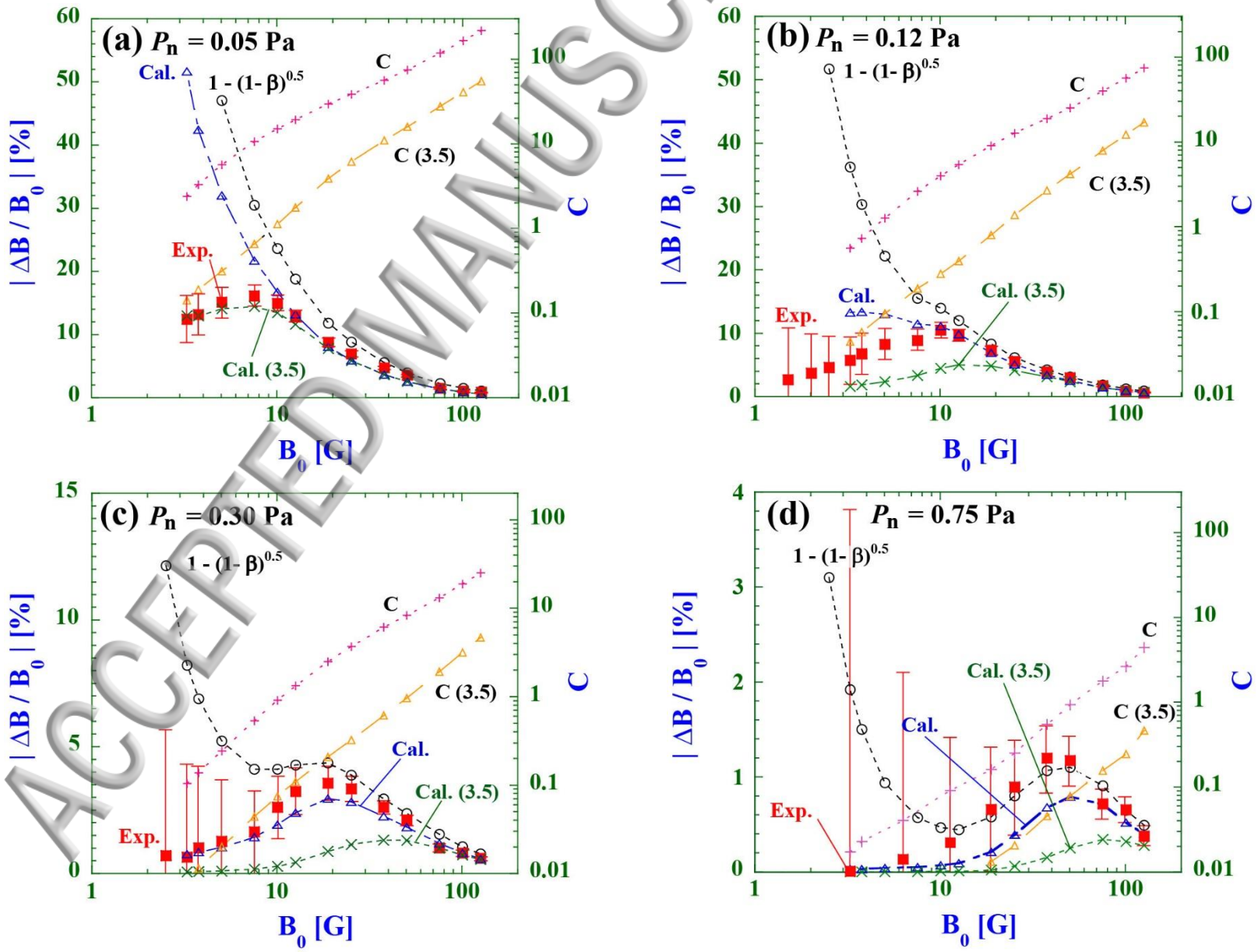

ACCEPTED MANUSCRIPT

Fig. 6

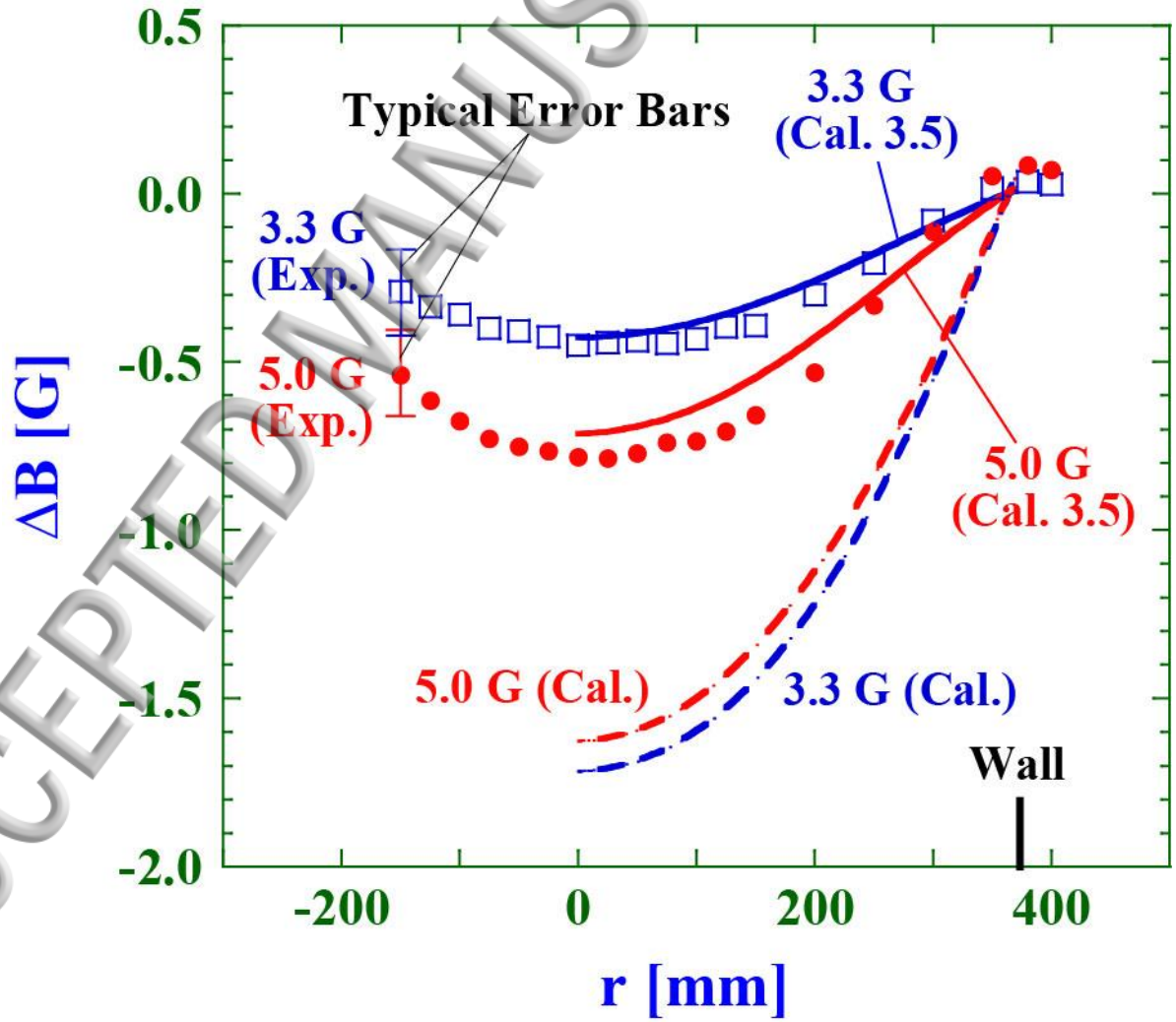

ACCEPTED MANUSCRIPT

Fig. 7